Journal of Power Sources 195 (2010) 175–180

Contents lists available at ScienceDirect

Journal of Power Sources

journal homepage: www.elsevier.com/locate/jpowsour

Short communication

Effect of precursor nature on the performance of palladium–cobalt electrocatalysts for direct methanol fuel cells

Alexey Serov[a,*], Tatyana Nedoseykina[b], Oleg Shvachko[b], Chan Kwak[a]

[a] Corporate R&D Center, Samsung SDI, Shin-dong 575, Yeongtong-gu, Suwon-si, Gyeonggi-do 443-731, South Korea
[b] Research Institute of Physics at Southern Federal University, Stachki Ave., 194, Rostov-on-Don 344090, Russia

ARTICLE INFO

Article history:
Received 1 October 2008
Received in revised form 23 June 2009
Accepted 26 June 2009
Available online 7 July 2009

Keywords:
Palladium
Cobalt
Fuel cell
Catalyst
ORR

ABSTRACT

The performance of platinum-free palladium–cobalt catalysts in oxygen reduction was investigated for a direct methanol fuel cell. The dependence of catalytic activity on precursor nature was determined for two classes of precursors; namely, palladium chloride and palladium nitrate. The nitrate precursor exhibits much higher catalytic performance than the chloride precursor. X-ray absorption fine structure (XAFS) spectra indicate that the structure of palladium catalyst prepared from nitrate is much closer to Pd_3Co structure that can explain high catalytic activity. The MEA prepared from the nitrate catalyst achieved the peak power density of 125 mW cm^{-2}, which is much higher than 19 mW cm^{-2} measured on the cell prepared from the chloride catalyst.

1. Introduction

The interest of researchers in fuel cells increases from year to year because fuel cells offer a cleaner and more efficient source of energy compared with other energy-conversion devices. Significant and careful investigations in the field of fuel cells may allow the energy converting devices to be commercialized soon. In the early days, research in the field of fuel cells addressed fundamental aspects, but now the emphasis has shifted from academic studies to commercial applications. One of the main problems with the commercial use of fuel cells is the high cost of materials such as a catalyst and stack components. The high price of platinum and platinum-based alloys is a major contributor to the final cost of a fuel cell.

All low temperature fuel cells, such as the polymer electrolyte membrane fuel cell (PEMFC) and the direct methanol fuel cell (DMFC), have used platinum or platinum alloys as electrode materials. Platinum possesses the highest catalytic activity and therefore it has been widely used in most fuel cell systems. On the other hand, the high price of platinum has accelerated the development of non-platinum materials. There have been many investigations of non-platinum catalysts for oxygen reduction, and there is a wide range of alternative materials that can substitute platinum. Ruthenium-based materials [1] and heat-treated macrocycles [2] are representative candidates; however, their activities in the oxygen reduction reaction (ORR) are too low to be alternatives to platinum.

Palladium has a similar valence shell electronic configuration and lattice constant to platinum. Considering both aspects of performance and price, palladium can be a good alternative material for low-temperature fuel cells. At present, spot price for troy ounce of palladium is practically five times lower than the same price for platinum, such a price difference is suitable for commercial uses of palladium or palladium alloys in fuel cell applications. Palladium is the most frequently employed catalyst material for anode reactions in formic acid fuel cells [3]. Recently, the indications of the high activity have appeared in the oxygen electroreduction, therefore attempts have been made to use palladium as an oxygen reduction catalyst with acidic electrolytes [4–8]. These researches have used palladium alloys with base metals in order to improve the performance of the oxygen reduction. A series of studies have shown that $CoPd_3$ is the most likely composition for the electrochemically active site for the oxygen reduction reaction on the family of bimetallic palladium catalysts [6–8].

It is widely accepted that the properties of metal catalysts are affected by several factors such as the condition of catalyst preparation, the nature of support, and the selection of metal precursor. In the course of developing palladium–cobalt catalysts, we have observed the precursor nature as the key factor in our preparation method. In this work, the aim has been to investigate the electrocat-

* Corresponding author. Present address: Paul Scherrer Institute, 5232 Villigen PSI, Switzerland. Tel.: +41 56 5345251; fax: +41 56 3104435.
E-mail addresses: alexey.serov@psi.ch, vores@mail.ru (A. Serov), tatianani@gmail.com (T. Nedoseykina), kcpmhkj@yahoo.com (C. Kwak).

0378-7753/$ – see front matter © 2009 Elsevier B.V. All rights reserved.
doi:10.1016/j.jpowsour.2009.06.087

alytic properties of palladium–cobalt from Pd chloride vs. those of palladium–cobalt from Pd nitrate. The palladium–cobalt catalysts prepared using different precursors are compared with cathode catalysts in single cell DMFC for ORR. Extended X-ray absorption fine structure (EXAFS) technique provided the information of local coordination and interatomic distances to propose a model of active species. Finally, we correlate the catalytic activity for oxygen reduction with the active species of the palladium–cobalt.

2. Experiment

2.1. Catalyst preparation

The palladium–cobalt catalysts were prepared by the following method. Briefly, a water solution of cobalt nitrate (99.999% trace metals basis) (Aldrich) was added to a solution of palladium precursor (palladium nitrate (purum, ~40% Pd basis) or palladium chloride (>99.9%) (Aldrich)) in atomic ratio of Pd:Co = 75:25. Solution of HNO_3 was added to adjust pH of the mixture to 2–4. Hydrazine in excess was added drop-wise under stirring. The mixture was stirred for 24 h at room temperature, after which the black solid was filtrated and washed with deionized water several times. Obtained wet powder was dried in vacuum at 120 °C for 3 h and heat treated in a hydrogen/nitrogen mixture (90% N_2 and 10% H_2) flow (300 ml min^{-1}) at 200 °C for 3 h. The prepared catalysts were marked as PdCo-N and PdCo-C, for palladium nitrate and palladium chloride precursors, respectively.

2.2. Rotating disk electrode

The oxygen reduction reaction on the prepared PdCo catalyst was studied using a rotating disk electrode. Working electrodes were prepared by mixing 11 mg of the PdCo electrocatalyst, 1.13 ml of water, and 1.13 ml of isopropyl alcohol. The mixture was sonicated before a small volume (13.1 μl) was applied onto a glassy carbon disk with a sectional area of 0.283 cm^2. After drying the droplet, at room temperature, 11.2 μl of a Nafion® monomer solution (0.5 wt.%, DuPont) was applied onto the film. The loading of catalyst on the electrode was 0.225 mg cm^{-2}. The experimental setup involved a three-electrode arrangement connected to a potentiostat/galvanostat (Autolab model PGSTAT30). The reference electrode was Ag/AgCl and the counter-electrode was a platinum mesh. The measured potential was converted to the potential with respect to the standard hydrogen electrode. The electrochemical reduction reactions were performed by rotating the catalyst-loaded electrodes at 2000 rpm at a scan rate of 10 mV s^{-1} in 50 ml of 0.5 M H_2SO_4 at 25 °C.

2.3. Characterization

Samples for transmission electron microscopy (TEM) were prepared by grinding and successive ultrasonic treatment in isopropyl alcohol for 1 min. A drop of the suspension was dried on a standard TEM sample grid covered with holey carbon film. Tecnai™ G^2TEM with FEG was used for observations. Images were recorded with a Multiscan camera. Material composition analysis was performed by energy dispersive X-ray (EDX) analysis.

XAFS spectra at Co and Pd K-edges of the samples were recorded at the 7C1 Electrochemistry beamline at PAL (Pohang accelerator laboratory) with ring current of 120–170 mA at 2.0 GeV. A Si (1 1 1) double-crystal monochromator, whose energy resolution is $\Delta E/E = 2 \times 10^{-4}$, was used with detuning to 75% in intensity to eliminate the high-order harmonics. The data acquisition system for XAFS comprised three ionization detectors measuring beam intensity of incidence I_0, transmitted I_t and transmitted through reference I_r. The reference channel was employed primarily for internal calibration of the edge positions by using a pure foil of the metals. Nitrogen gas was used in the I_0, I_t and I_r chambers. The computer program used for the analysis of the XAFS data was the IFFEFIT [9,10]. Fourier transformation of EXAFS oscillations with different k-weight was carried out in k-range from 2.5 to 12.1 $Å^{-1}$ for the Co spectra and from 2.6 to 13.7 $Å^{-1}$ for the Pd spectra for both samples. Fitting was done in R-space in range from 1.65 to 3.16 Å for the Co spectra and from 1.56 to 3.00 Å for the Pd spectra.

2.4. Single cell test

The membrane electrode assemblies (MEAs) were fabricated by spraying the catalyst ink (measured amount of catalyst was homogenized in iso-propanol:water mixture 90:10%) onto Nafion® 112. The anode catalyst is PtRu black (Johnson Matthey, 4.0 mg cm^{-2}) and the cathode catalysts are PdCo-C or PdCo-N black (3.4–3.7 mg cm^{-2}). The Nafion® content is 18 wt.% in both anode and cathode. The catalyst-coated membrane was sandwiched between the anode gas diffusion layer (GDL, SGL 10AC) and the cathode GDL (SGL 31BC) and then the assemblies were hot-pressed under a specific load of 140 kgf cm^{-2} for 3 min at 125 °C.

Polarization curves were obtained by the Wonatech testing system using a homemade single cell with a working area of 10 cm^2. Methanol solution (1 M) was fed to the anode side of the cell (anode stoichiometry = 3) while dry air was fed to the cathode side (cathode stoichiometry = 3) under atmospheric pressure. The single cell was operated at 80 °C.

3. Results and discussion

3.1. Influence of precursors on material morphology

The composition of the PdCo-N and PdCo-C catalysts was determined by EDX analysis. It was found that an average composition of Pd and Co in these samples was in the atomic ratio ranges of 74:26 and 72:28, respectively. As it clearly can be seen from TEM images (Fig. 1a and b) materials morphology is different for the two types of catalysts. In case of PdCo-N uniform distribution of catalyst particles can be achieved, whereas PdCo-C has large zones of agglomerated particles. It can be estimated that an average particle size for PdCo-N is in the range of 10–12 nm, while PdCo-C particles are about 16–19 nm. As it was shown before [11] for palladium catalysts, even supported on carbon, formation of large particles is preferable. Such significant difference in particle size for the catalysts prepared from two types of precursors can be explained by reduction mechanism. It was reported [12] that in water solution with pH > 1–2 palladium nitrate forms colloid suspension of PdO, with fine particles as low as 1.8–2 nm. During the addition of hydrazine to the mixture of palladium nitrate and cobalt nitrate, pH of the solution changed from acidic to basic, with precipitation of cobalt hydroxide. Active PdO particles can be easily reduced with hydrazine and can be adsorbed on the surface of cobalt hydroxide in solution. In this case agglomeration on the stage of preliminary alloy formation can be avoided. On the contrary, Yang et al. [13] showed that the presence of Cl^- ions promotes significant growth of palladium particles, so even before the heat treatment procedure particles in solution in the case of palladium chloride precursors are larger in comparison with palladium nitrate. This assumption can be confirmed by visual observation in color difference between the two powders, obtained after reduction by hydrazine. PdCo-N was black while PdCo-C had a grey color. After heat treatment this difference in color remained the same.

3.2. Influence of precursors on alloy structure

As a result of investigations in the field of palladium-alloy catalyst for fuel cell application, it was supposed that the second metal

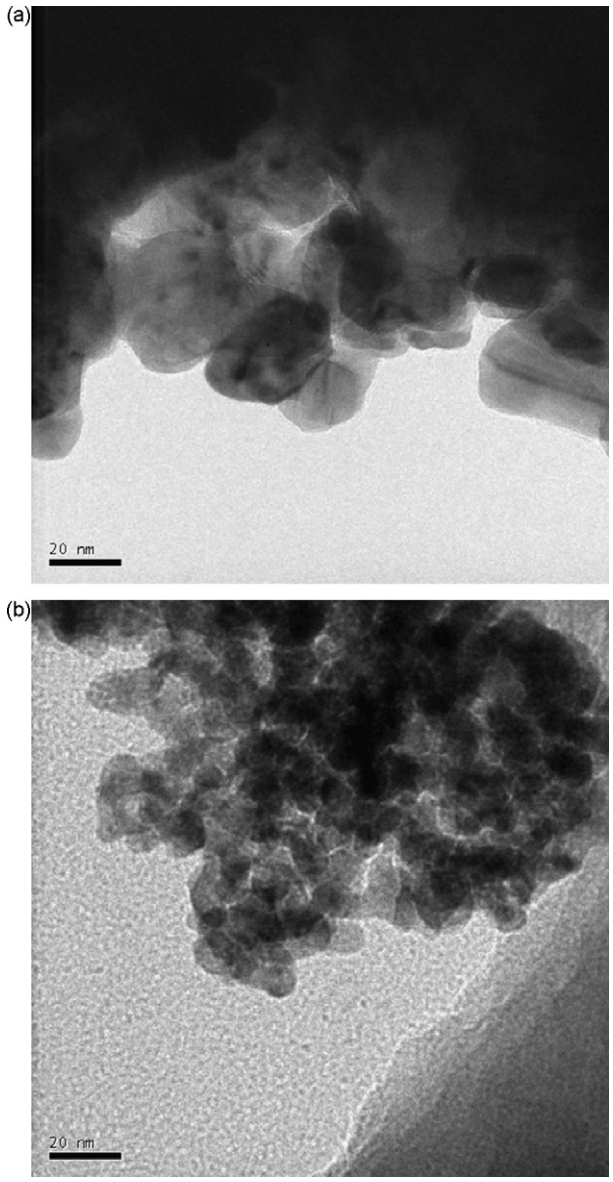

Fig. 1. TEM image of unsupported PdCo synthesized from (a) chloride precursor (PdCo-C) and (b) nitrate precursor (PdCo-N).

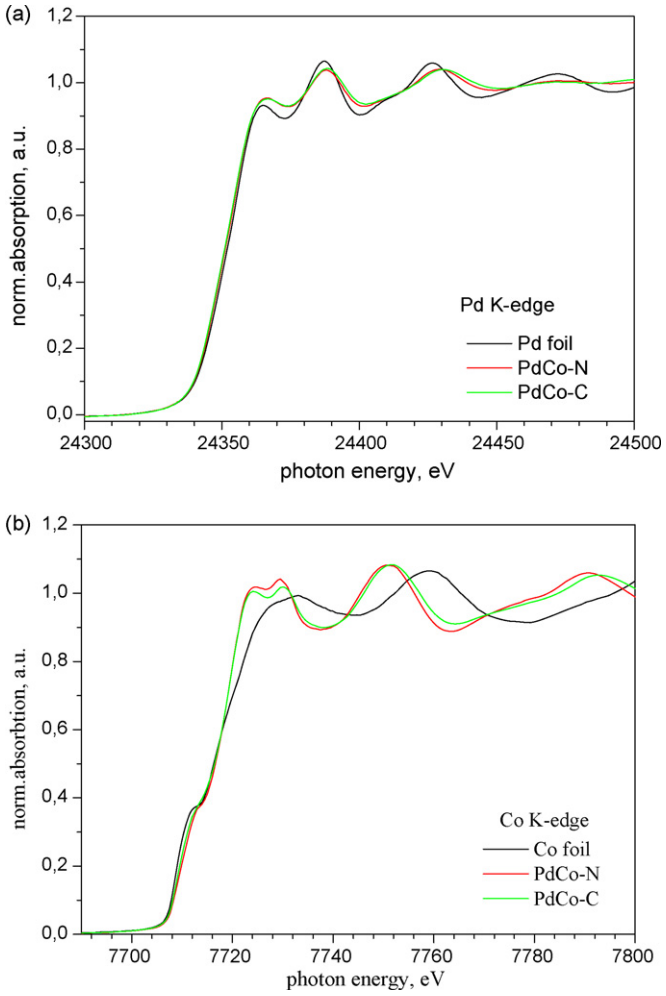

Fig. 2. (a) Pd and (b) Co K-edge XANES of PdCo-nanoparticles and Pd foil.

can enhance catalytic activity in ORR by a different mechanism. It includes a hypothesis dealing with change in the density of states (DOS) at the Fermi level of Pd sites by alloy formation [14], facilitated O_2 dissociation by alloy formation [15], formation of the desirable "Pd shell and alloy core" structure [16], etc. In order to explain the effect of precursors on alloy structure and further catalytic activity X-ray absorption fine structure (XAFS) technique has been used.

The Co and Pd K-edges XANES spectra of the samples and references are presented in Fig. 2a and b. The first peak after absorption edge in each Pd K-edge spectrum corresponds to the allowed 1s–5p transition and is directly related to the occupancy of 5d electronic states. It is seen from Fig. 2a that the Pd K-edge XANES spectra of the samples are almost the same and slightly different from that of the Pd metal, which exhibited an fcc structure. This difference deals with nanosized nature of sample and also additive Co metal affects on the Pd local structure. The last follows from noticeable changes in magnitudes and phases of the EXAFS oscillations in the spectra of the samples as compared to the Pd metal spectrum.

The Co K-edge XANES spectra of the samples are similar to each other and significantly different from that of the Co metal owned by hcp structure (Fig. 2b). The last result is expected because in the alloys the Co atoms are almost surrounded by noble metal atoms that strongly change the Co K-edge XANES spectrum [17]. In this case as it follows from the simulated and experimental Co K-edge spectra the first peaks after the absorption edge corresponding 1s–4d electron transitions shift toward a small energy [17]. Energy distance between the peaks is around 4.9 and 5.8 eV for the PdCo-N and PdCo-C, respectively, while for the Co metal the splitting of the peaks is ill-defined and equals to 3.7 eV. The shift of the first peak with regard to the absorption edge corresponds to 7.8 eV for both samples, whereas 12.7 and 13.7 eV corresponds to the shift of the second peak for the PdCo-N and PdCo-C, respectively. The comparison of the cobalt spectra for the studied bimetallic nanoparticles with simulated ones in [17] results in a preliminary conclusion that the Co atoms correspond to the fcc structure of noble metal atoms.

Fourier transforms (FT) of the Pd and Co K-edges EXAFS spectra presented in Fig. 3a and b demonstrate two well resolved peaks at 1.98, 2.45 and 2.08, 2.45 Å, respectively. To understand these figures we first considered the FT of theoretically calculated Pd and Co K-edges EXAFS of Pd_3Co alloy as far as the synthesis condition predicts the structure formation. The structure of Pd_3Co is $Pm\bar{3}m$ with $a = 3.820$ Å [18]. In the model structure the nearest neighbors of Co are 12 Pd atoms at $R = 2.701$ Å and 6 Co atoms at $R = 3.82$ Å. The local environment of Pd composes of 4 Co and 8 Pd atoms at $R = 2.701$ Å and 6 Pd at $R = 3.82$ Å. For the described structure

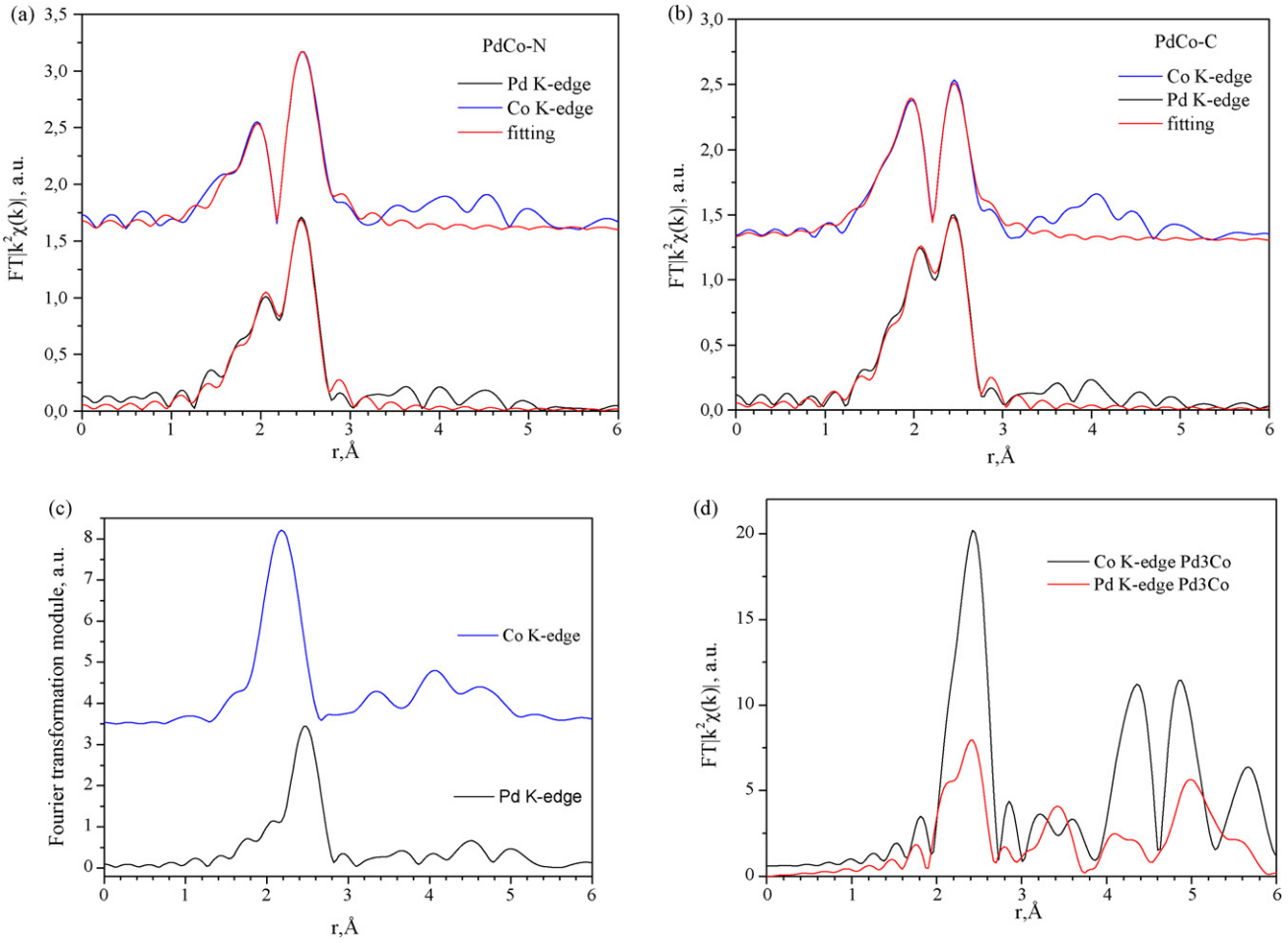

Fig. 3. Fourier transformations of the experimental $k^2\chi(k)$ Pd and Co K-edge EXAFS of PdCo-nanoparticles (a and b) and references (c) and the model $k^2\chi(k)$ Pd and Co K-edge EXAFS of Pd_3Co (d).

FT of both edges EXAFS should look like these in Fig. 3c. A single peak at 2.45 Å in both FTs corresponds to the Pd–Co/Pd and Co–Pd coordination shells. This peak is also observed in FT of both edges EXAFS spectra of the studied samples. The additional peaks at 1.98 and 2.08 Å can be found in the experimental FT of the samples for Co and Pd, respectively. The appearance of the peak in the Co FT can be dealt with Co–Co interactions originated probably due to Co nanoparticles formation or Co thin layer on Pd nanoparticles or any aggregation of Co in the PdCo-nanoparticles. The peak at 2.08 Å in the Pd FT may be indicative of the coexisting of Pd_3Co and the additional Pd phases. This assumption can be confirmed by the different magnitudes ratio of the first peak to the second one in the Co and Pd FTs.

To obtain more information about the local atomic structure of the Co and Pd in the studied materials it was carried out a fitting for two first peaks of FT. Both the Co and Pd spectra fitted simultaneously by using the structure of Pd_3Co as initial one. EXAFS fits performed simultaneously in *k*-weightings of one, two and three to avoid introducing errors with regard to the coordination numbers and Debye–Waller factors. The obtained result required including the additional Co–Co and Pd–Pd contributions. Table 1 shows the best fitting data for the samples and for the Pd, Co references. Agreement between the experimental and model FTs for the samples is presented in Fig. 3a and b.

For both samples the Pd–Pd and Pd–Co coordination numbers (CN) are 12 that indicates the formation of large bimetallic particles in which Pd is diluted by cobalt metal atoms. The Co–Pd CN is different for two samples by 1.5 times. In case of PdCo-N, the CN well corresponds to the structure with atomic ratio Pd:Co 3:1. For PdCo-C it is rather 1:1, i.e. PdCo.

In Table 1 it is noted a decrease in the Pd–Pd interatomic distances in both samples, compared to Pd metal, while the Pd–Co bond distances are even smaller. This indicates shrinkage of the Pd crystalline structure, this being one of the effects of the incorporation of metal atom with smaller radius in the Pd fcc structure. The Pd–Co bond distances in the nanoparticles of both samples are near arithmetic-mean value of Pd–Pd (2.75 Å) and Co–Co (2.50 Å) distances in Pd and Co metals, respectively. It is obvious that the value of the distance depends on the atomic ratio Pd:Co: than larger CN of the Co–Co shell than shorter all the distances (PdCo-C). It is worth to point out that for both samples the Co–Co bond distance is larger than this in the Co metal. It can be evidence of absence of the Co segregation in the materials. These results are in good agreement with our preliminary conclusion made based on XANES analysis that the Co atoms are in fcc structure and coordinated by the noble metal atoms. The structural data presented here for the nanoparticles are very similar to those observed in other bimetallic nanoparticles PtCo, PtCr, PtV, PdCu and PdCo [19–23].

3.3. *Influence of precursors on catalytic properties*

Catalytic activity of alloyed materials strongly depends on catalyst morphology, particle size and distribution, and electronic interaction between alloyed metals. There are several factors which can be used to achieve highest catalytic activity: selection of reduction agent, heat treatment conditions, different support materials,

Table 1
Interatomic distance *R*, coordination number *N*, mean-square relative displacement of the interatomic distance for each bond pair σ^2 and Rf-factor of fit (characterizes differences between theoretical and experimental data) determined from the analysis of EXAFS data of the PdCo-nanoparticles and references.

Sample	Co–Co			Co–Pd			
	R, Å	*N*	σ^2, Å^2	*R*, Å	*N*	σ^2, Å^2	Rf, %
Co foil	2.4988 ± 0.0018 2.5106 ± 0.0018	6 6	0.0062 0.0063				
PdCo-N	2.5782 ± 0.0280	1.4 ± 0.7	0.0041 ± 0.0050	2.6318 ± 0.012	8.9 ± 0.7	0.0090 ± 0.0011	0.5
PdCo-C	2.5635 ± 0.0083	4.2 ± 0.8	0.0113 ± 0.0026	2.6175 ± 0.0053	6.2 ± 0.4	0.0084 ± 0.0005	0.3
Sample	Pd–Pd			Pd–Co			Rf, %
	R, Å	*N*	σ^2, Å^2	*R*, Å	*N*	σ^2, Å^2	
Pd foil	2.7497	12	0.0058				
PdCo-N	2.7108 ± 0.0051	8.8 ± 0.7	0.0060 ± 0.0005	2.6318 ± 0.0120	3.5 ± 0.6	0.0090 ± 0.0011	0.5
PdCo-C	2.7041 ± 0.0029	7.8 ± 0.4	0.0062 ± 0.0005	2.6175 ± 0.0053	4.6 ± 0.3	0.0084 ± 0.0005	0.3

etc. In the present research we found that nature of the selected precursor has a great influence on the final catalytic activity. Two palladium–cobalt catalysts prepared from palladium nitrate and palladium chloride precursors were tested in reaction of oxygen reduction in acid media. RDE data for both catalysts are shown in Fig. 4. It can be concluded from RDE data that catalytic activity in case of PdCo-N is considerably higher than that of PdCo-C catalysts. Such an effect can be well explained by particle size difference (TEM) and by different crystal and electronic structure (XAFS). One of the possible explanations of increasing catalytic activity in case of PdCo catalysts in comparison with pure palladium is Pd lattice compression due to alloy formation. Such a lattice compression accompanied with reduction of Pd–Co bonds results in the shift of d-band center, which has an effect on surface activity of Pd sites. It was shown by DFT calculations that the compression of a Pd lattice in alloys produces the downshift of the d-band center energy [24]. The data obtained in the present research showed bonds reduction in prepared palladium–cobalt catalysts and fully confirmed results of DFT calculations. PdCo alloy prepared from nitrate precursor has Pd–Co distance closer to preferable Pd_3Co structure in contrast to PdCo made from chloride precursor. Such a difference should significantly affect on catalytic activity.

The series of experiments with MEAs prepared using PdCo-C and PdCo-N as cathode catalysts were performed. Results of the single-cell performance of both catalysts made from different precursors are shown in Fig. 5. MEA prepared from PdCo-N achieves the peak power density of 125 mW cm^{-2}, while PdCo-C shows only

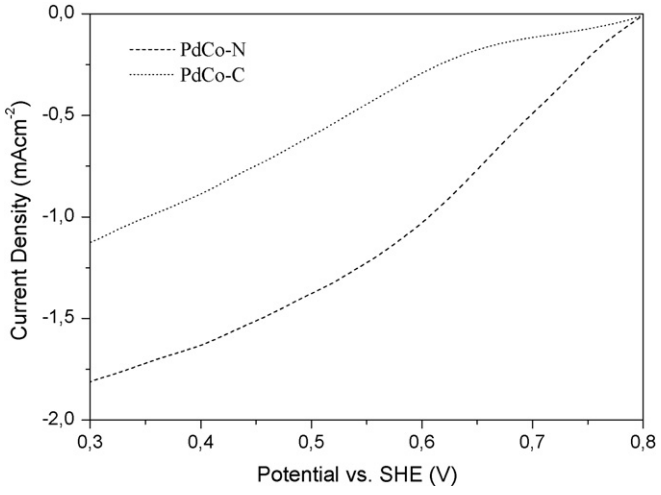

Fig. 4. Steady-state polarization curves for oxygen reduction in 0.5 M. H_2SO_4 solution on a RDE prepared with PdCo-C (dots) and PdCo-N (dashes) catalysts.

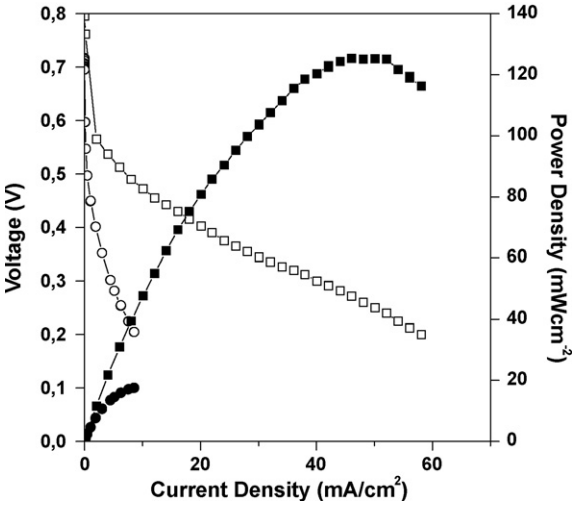

Fig. 5. The polarization curves and power density curves of single cells with PdCo-N (square) and PdCo-C (circle). Fuel: 1 M methanol (stoichiometry = 3); oxidant: air under atmospheric pressure (stoichiometry = 3); temperature: 80 °C.

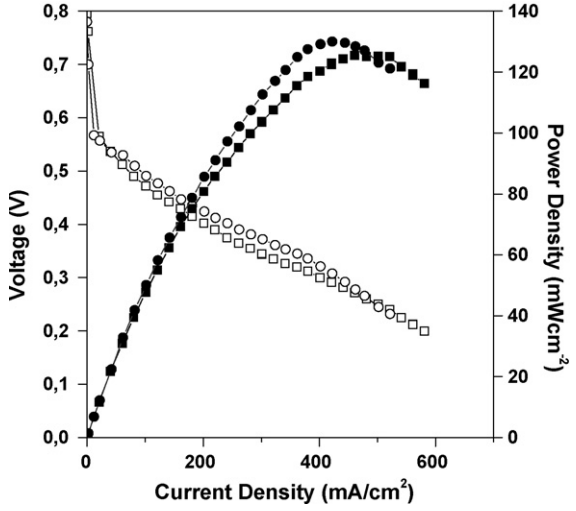

Fig. 6. The polarization curves and power density curves of single cells with PdCo-N (square) and commercial MEA (anode: PtRu black, 4.1 mg cm^2, cathode Pt black, 3.5 mg cm^{-2}) (circle). Fuel: 1 M methanol (stoichiometry = 3); oxidant: air under atmospheric pressure (stoichiometry = 3); temperature: 80 °C.

19 mW cm^{-2}. The possible explanation of such a significant difference in activity can be made by taking into account the different morphology and electronic structures of these catalysts. It should be mentioned that value of 125 mW cm^{-2} is the highest for non-platinum catalysts and can be compared with power density of a commercial MEA prepared using platinum cathode (see Fig. 6). It was shown that the performance of palladium–cobalt catalyst was comparable with that of the platinum catalyst. On the contrary, additional efforts are required for the substitution of platinum by PdCo catalysts, namely experiments with durability and stability of new palladium–cobalt catalysts.

4. Conclusions

It can be concluded from the above experimental observations and discussion that selection of precursor for the preparation of palladium–cobalt alloys can significantly affect the final catalytic activity. The influence of precursor can be explained by difference in catalysts morphology and electronic structure. It was clearly shown that nitrate precursor is more preferable than chloride. PdCo prepared from nitrate precursor shows fine particles distribution with average particle size of 10–12 nm. As a result of the combination of above-mentioned characteristics the prepared catalyst possesses high catalytic activity in comparison with PdCo prepared from chloride precursor. The maximum power density achieved with PdCo-N is 125 mW cm^{-2}. This value is comparable with power density for commercial MEAs and allows to use new catalyst in future fuel cell systems instead of platinum.

References

[1] M. Hilgendorff, K. Diesner, H. Schulenburg, P. Bogdanoff, M. Bron, S. Fiechter, J. New Mater. Electrochem. Syst. 5 (2002) 71–81.
[2] M. Lefevre, J.P. Dodelet, P. Bertrand, J. Phys. Chem. B 104 (2000) 11238–11247.
[3] R.S. Jayashree, J.S. Spendelow, J. Yeom, C. Rastogi, M.A. Shannon, P.J.A. Kenis, Electrochim. Acta 50 (2005) 4674–4682.
[4] O. Savadogo, K. Lee, K. Oishi, S. Mitsushima, N. Kamiya, K.-I. Ota, Electrochem. Commun. 6 (2004) 105–109.
[5] W. Wang, D. Zheng, C. Du, Z. Zou, X. Zhang, B. Xia, H. Yang, D.L. Akins, J. Power Sources 167 (2007) 243–249.
[6] W.E. Mustain, K. Kepler, J. Prakash, Electrochem. Commun. 8 (2006) 406–410.
[7] W.E. Mustain, J. Prakash, J. Power Sources 170 (2007) 28–37.
[8] W.E. Mustain, K. Kepler, J. Prakash, Electrochim. Acta 52 (2007) 2102–2108.
[9] B. Ravel, M. Newville, J. Synchrotron Radiat. 12 (4) (2005) 537–541.
[10] M. Newville, J. Synchrotron Radiat. 8 (2001) 322–324.
[11] A.A. Serov, S.-Y. Cho, S. Han, M. Min, G. Chai, K.H. Nam, C. Kwak, Electrochem. Commun. 9 (2007) 2041–2044.
[12] B. Didillon, E. Merlen, T. Pagès, D. Uzio, Stud. Surf. Sci. Catal. 118 (1998) 41.
[13] Y. Yang, Y. Zhou, C. Cha, W.M. Carroll, Electrochim. Acta 38 (1993) 2333–2341.
[14] K. Lee, O. Savadogo, A. Ishihara, S. Mitsushima, N. Kamiya, K.-I. Ota, J. Electrochem. Soc. 153 (1) (2006) A20–A24.
[15] J.L. Fernandez, D.A. Walsh, A.J. Bard, J. Am. Chem. Soc. 127 (2005) 357–365.
[16] Y. Suo, L. Zhuang, J. Lu, Angew. Chem. Int. Ed. 46 (2007) 2862–2864.
[17] F. Zeng, R.L. Zong, Y.L. Gu, F. Lv, F. Pan, J. Wang, W.S. Yan, B. He, Y.N. Xie, T. Liu, Nucl. Instrum. Methods Phys. Res. B 260 (2007) 547–552.
[18] N.P. Lyakishev, O.A. Bannyh, L.L. Rohlin, Handbook "State Diagram of Bimetal Systems", 1996.
[19] F.H.B. Lima, M.J. Giz, E.A. Ticianelli, J. Braz. Chem. Soc. 16 (2005) 328.
[20] J. Batista, A. Pintar, J.P. Gomilšek, A. Kodre, F. Bornette, Appl. Catal. A: Gen. 217 (2001) 55–68.
[21] B. Mierzwa, Z. Kaszkur, B. Moraweck, J. Pielaszek, J. Alloys Compd. 286 (1999) 93–97.
[22] B. Mierzwa, J. Alloys Compd. 362 (2004) 178–188.
[23] B. Mierzwa, J. Alloys Compd. 401 (2005) 127–134.
[24] B. Hammer, J.K. Norskov, Adv. Catal. 45 (2000) 71–129.